

# JGR Atmospheres

## RESEARCH ARTICLE

10.1029/2019JD031128

### Key Points:

- Water-soluble ions showed substantial difference for saline mineral dust samples collected in different regions in China
- Large variation in hygroscopicity of saline mineral dust was found, largely depending on their chemical composition
- Measured hygroscopic growth factors agreed reasonably well with those predicted using ISORROPIA-II for saline mineral dust

### Supporting Information:

- Supporting Information S1

### Correspondence to:

M. Tang,  
mingjintang@gig.ac.cn

### Citation:

Tang, M., Zhang, H., Gu, W., Gao, J., Jian, X., Shi, G., et al. (2019). Hygroscopic properties of saline mineral dust from different regions in China: Geographical variations, compositional dependence, and atmospheric implications. *Journal of Geophysical Research: Atmospheres*, 124, 10,844–10,857. <https://doi.org/10.1029/2019JD031128>

Received 4 JUN 2019

Accepted 3 SEP 2019

Accepted article online 13 SEP 2019

Published online 18 OCT 2019

## Hygroscopic Properties of Saline Mineral Dust From Different Regions in China: Geographical Variations, Compositional Dependence, and Atmospheric Implications

Mingjin Tang<sup>1,2,3</sup> , Huanhuan Zhang<sup>1,2</sup>, Wenjun Gu<sup>1,2</sup>, Jie Gao<sup>4</sup>, Xing Jian<sup>5</sup> , Guoliang Shi<sup>4</sup>, Bingqi Zhu<sup>6</sup> , Luhua Xie<sup>7</sup>, Liya Guo<sup>1,2</sup>, Xiaoyan Gao<sup>1</sup> , Zhe Wang<sup>8</sup> , Guohua Zhang<sup>1</sup> , and Xinming Wang<sup>1,2,3</sup> 

<sup>1</sup>State Key Laboratory of Organic Geochemistry and Guangdong Key Laboratory of Environmental Protection and Resources Utilization, Guangzhou Institute of Geochemistry, Chinese Academy of Sciences, Guangzhou, China,

<sup>2</sup>University of Chinese Academy of Sciences, Beijing, China, <sup>3</sup>Center for Excellence in Regional Atmospheric Environment, Institute of Urban Environment, Chinese Academy of Sciences, Xiamen, China, <sup>4</sup>State Environmental Protection Key Laboratory of Urban Ambient Air Particulate Matter Pollution Prevention and Control, College of Environmental Science and Engineering, Nankai University, Tianjin, China, <sup>5</sup>State Key Laboratory of Marine Environmental Science, College of Ocean and Earth Sciences, Xiamen University, Xiamen, China, <sup>6</sup>Key Laboratory of Water Cycle and Related Land Surface Processes, Institute of Geographic Sciences and Natural Resources Research, Chinese Academy of Sciences, Beijing, China, <sup>7</sup>Key Laboratory of Ocean and Marginal Sea Geology, Guangzhou Institute of Geochemistry, Chinese Academy of Sciences, Guangzhou, China, <sup>8</sup>Department of Civil and Environmental Engineering, The Hong Kong Polytechnic University, Kowloon, Hong Kong

**Abstract** Saline mineral dust particles, emitted from saline topsoil in arid and semiarid regions, contribute significantly to tropospheric aerosol particles. However, hygroscopic properties of saline mineral dust particles, especially for those found in regions other than North America, are poorly understood. In this work we investigated hygroscopic properties of 13 saline mineral dust samples collected from different locations via measuring sample mass change at different relative humidity (RH; up to 90%), and measured their chemical and mineralogical compositions using ion chromatography and X-ray diffraction. The mass growth factors at 90% RH, defined as the sample mass at 90% RH relative to that at <1% RH, were found to display large geographical variations, spanning from ~1.02 to 6.7, and the corresponding single hygroscopicity parameters ( $\kappa$ ) were derived to be in the range of <0.01 to >1.0. The saline components (mainly  $\text{Na}^+$ ,  $\text{Cl}^-$ , and  $\text{SO}_4^{2-}$ ) contained by saline mineral dust particles largely determined their hygroscopicity, and the predicted mass growth factors at 90% RH using an aerosol thermodynamic model (ISORROPIA-II), agreed with measured values within 20% for most of samples examined, although larger discrepancies also occurred for three samples. Our results improve our understanding in hygroscopicity of saline mineral dust particles and thus their heterogeneous chemistry and ability to serve as cloud condensation nuclei to form cloud droplets.

## 1. Introduction

Mineral dust aerosol, emitted from arid and semiarid areas with a flux of around 2,000 Tg per year, is one of the major types of aerosol particles in the troposphere (Ginoux et al., 2012; Huneeus et al., 2011; Textor et al., 2006) and has significant impacts on air quality, radiative forcing, and biogeochemical cycles. It scatters and absorbs solar and terrestrial radiation (Balkanski et al., 2007; Chen et al., 2017; Di Biagio et al., 2017; Huang et al., 2015), and affects the formation and properties of clouds as well as precipitation via serving as cloud condensation nuclei (CCN; Karydis et al., 2017; Kumar et al., 2011; Tang et al., 2016) and ice-nucleating particles (Creamean et al., 2013; Cziczo et al., 2013; Murray et al., 2012; Tang et al., 2016). Heterogeneous reactions of mineral dust aerosol would significantly change the abundance of reactive trace gases in the troposphere and also contribute to the formation of secondary particulate matters, such as nitrate and sulfate (Dupart et al., 2012; He et al., 2014; Laskin et al., 2005; Li & Shao, 2009; Romanias et al., 2016; Tang et al., 2017; Usher et al., 2003; Wang et al., 2013; Zhang & Iwasaka, 1999). Furthermore, deposition of mineral dust is known to be an important source of Fe and P in open oceans, largely controlling biogeochemical cycles in these regions (Conway & John, 2014; Jickells et al., 2005; Li et al., 2017; Mahowald et al., 2011; Mahowald et

al., 2018). Dust particles are mainly composed of minerals with low hygroscopicity, including quartz, feldspar, carbonate, iron oxides, illite, kaolinite, and montmorillonite (Engelbrecht et al., 2016; Formenti et al., 2011; Ito & Wagai, 2017; Journet et al., 2014; Nickovic et al., 2012; Rodriguez-Navarro et al., 2018; Shao et al., 2007). Therefore, fresh mineral dust particles are usually considered to be rather nonhygroscopic, and the single hygroscopicity parameters,  $\kappa$ , are typically found to be smaller than 0.01 (Herich et al., 2009; Koehler et al., 2009; Ma et al., 2010; Sullivan et al., 2009; Tang et al., 2016).

In addition to minerals with low hygroscopicity, mineral dust particles, especially for those emitted from playas (i.e., dry lakebeds), may contain substantial amount of soluble materials (Abuduwaili et al., 2008; Abuduwaili et al., 2010; Gillette et al., 1992). For example, in the area of Lake Ebinur (Xinjiang, China), deposited aerosol particles were found to contain 10–25% of soluble salts by mass. In fact, despite their relatively small geographical coverage, playas have been identified as an important source of mineral dust aerosol over the globe (Gill, 1996; Prospero et al., 2002). Due to increasing demand in water and climate change, lakes in arid and semiarid regions, such as the Aral Sea and the Caspian Sea, are shrinking, and therefore, mineral dust aerosol emitted from playas may become more important in the future. In addition to playa soils, normal soil in arid and semiarid regions also contain some amount of soluble materials (Wang et al., 2012; Zhu, 2016a, 2016b). For example, the mass fraction of soluble salts were found to range from 0.28% to 14.78% for surface materials collected in the Gobi desert (Wang et al., 2012), and sulfate, which was suggested to derive directly from soil, could contribute to about 4% to particle mass during a dust storm event at the Taklimakan desert (Wu et al., 2012). Although the salinity of normal soil can be much lower than playa soil, it can be a very important source for aeolian soluble materials due to its much larger geographical coverage.

The presence and impacts of saline mineral dust aerosol, though much less explored when compared to normal mineral dust, have been recognized by a number of studies. Playa-derived materials were identified in Saharan dust plumes over the Atlantic (Formenti et al., 2003), and analysis of individual aerosol particles collected in Beijing during a dust storm revealed that some particles were enriched in S, Cl, and Na (Zhang et al., 2009), very likely to derive from playas and saline soils. In fact, two Asian dust reference samples were found to contain significant amount of water-soluble materials (Osada, 2013). Another study (Blank et al., 1999) suggested that aeolian dust over a saline playa in Nevada (USA) contained substantial amount of water-soluble ions. Residues of cloud droplets in orographic wave clouds over Wyoming (USA) were found to contain soluble inorganic salts (Pratt et al., 2010), indicating that saline mineral dust particles emitted from playas may play an important role in cloud formation in continental regions with limited marine influence. Saline mineral dust emitted from soil in western United States and Mexico may contribute significantly to particulate  $\text{Na}^+$  and  $\text{Cl}^-$  observed in Colorado (USA), although its contribution relative to the marine source remained to be precisely differentiated (Jordan et al., 2015). A recent study (Frie et al., 2017) concluded that saline dust emitted from playas could contribute 8.9% to the daily  $\text{PM}_{10}$  mass for coastal regions along the Salton Sea (California, USA). Furthermore, saline mineral dust aerosol was also observed in many other regions, such as Argentina (Bucher & Stein, 2016) and Iran (Gholampour et al., 2015), indicating its global occurrence.

Despite important roles that saline mineral dust aerosol may play, hygroscopic properties of saline mineral dust from different sources, as only explored in a few previous studies (Gaston et al., 2017; Koehler et al., 2007; Pratt et al., 2010), remain poorly understood, precluding an in-depth understanding of its environmental and climatic effects. Koehler et al. (2007) investigated hygroscopic growth and cloud condensation nucleation of saline mineral dust particles collected from topsoil in the Owen Lake region (California, USA), and found that submicron dust particles consisted of at least two types of particles with distinct hygroscopicity. In a following study, Pratt et al. (2010) examined the CCN activity of dust particles collected from the surface of Owens Lake, and the average  $\kappa$  value was measured to be  $0.84 \pm 0.10$ . Very recently, Gaston et al. (2017) measured CCN activities of several saline mineral dust samples originating from different regions in southwestern and western United States. The measured  $\kappa$  values displayed large variation, ranging from  $0.002 \pm 0.001$  to  $0.818 \pm 0.094$ , and good correlation between hygroscopicity and mass fractions of soluble materials was observed (Gaston et al., 2017). It can be expected that saline mineral dust from different regions would have various salinity and thus exhibit different hygroscopicity. However, as discussed above, only a very limited number of previous studies have examined hygroscopicity of saline mineral dust samples from North American, and hygroscopic properties and CCN activities of saline mineral dust samples from

**Table 1**  
Overview of Mineral Dust Samples Examined in This Work

Province	Sample	Geographical coordinates	Further information
Xinjiang	XJ-1	N. A.	GBW07449
	XJ-2	N. A.	GBW07450
	XJ-3	92°49'17"E, 43°36'32"N	Playas topsoil
	XJ-4	91°11'14"E, 42°39'54"N	Playas topsoil
	XJ-5	89°14'42"E, 42°41'18"N	Playas topsoil
	XJ-6	91°31'3"E, 42°37'16"N	Playas topsoil
Inner Mongolia	IM-1	N. A.	GBW07447
	IM-2	101°23'10"E, 41°59'38"N	Playas topsoil
	IM-3	105°41'51"E, 38°50'42"N	Playas topsoil
Qinghai	QH	N. A.	GBW07448
Ningxia	NX	105°0'33"E, 37°38'38"N	Playas topsoil
		N	
Shaanxi	SX	N. A.	GBW07454
Shandong	SD	118°58'39"E, 37°45'36"N	Agricultural topsoil
		N	

Note. XJ-1, XJ-2, IM-1, QH, and SX are certificated reference materials provided by Chinese Academy of Geological Sciences, and the exact geographical locations where they were collected are not provided.

other regions are unknown. As a result, knowledge of hygroscopicity of saline dust from other major mineral dust aerosol sources is highly valuable.

Arid and semiarid areas are widely distributed in north and northwest China, being a globally important source of mineral dust aerosol (Ginoux et al., 2012; Huang et al., 2014; Zhang et al., 2003). To further understand physicochemical properties of saline mineral dust and its environmental and climatic impacts, in this work we investigated hygroscopic properties of 13 saline mineral dust samples originating from different locations in China. Mineralogical and chemical compositions of these samples were measured to examine the compositional dependence of hygroscopic properties. In addition, we compared our measured hygroscopic growth to that predicted using a thermodynamic model. The atmospheric implications of our work are also discussed.

## 2. Methodology

### 2.1. Sample Collection and Preparation

Thirteen saline mineral dust samples in total, originating from six different provinces in China, were investigated in this work. General information of these samples is given in Table 1, and locations where these samples were collected are displayed in Figure 1. Five samples were certificated reference materials provided by Chinese Academy of Geological Sciences, and the corresponding certificate numbers (e.g., GBW07449) can be found in Table 1. Another seven samples were collected from

playas topsoil, and the last sample was collected from agricultural topsoil in the Yellow River Delta.

The following procedure was used to process the eight topsoil samples we collected: (i) topsoil samples were first baked in an oven at 120 °C for 24 hr and then manually ground; (ii) they were sieved to remove particles larger than 1 mm, and then ground in a ball mill until most particles were smaller than 74 μm; (iii) the samples were baked again in an oven at 120 °C for 24 hr; and (iv) after these samples were cooled down, they

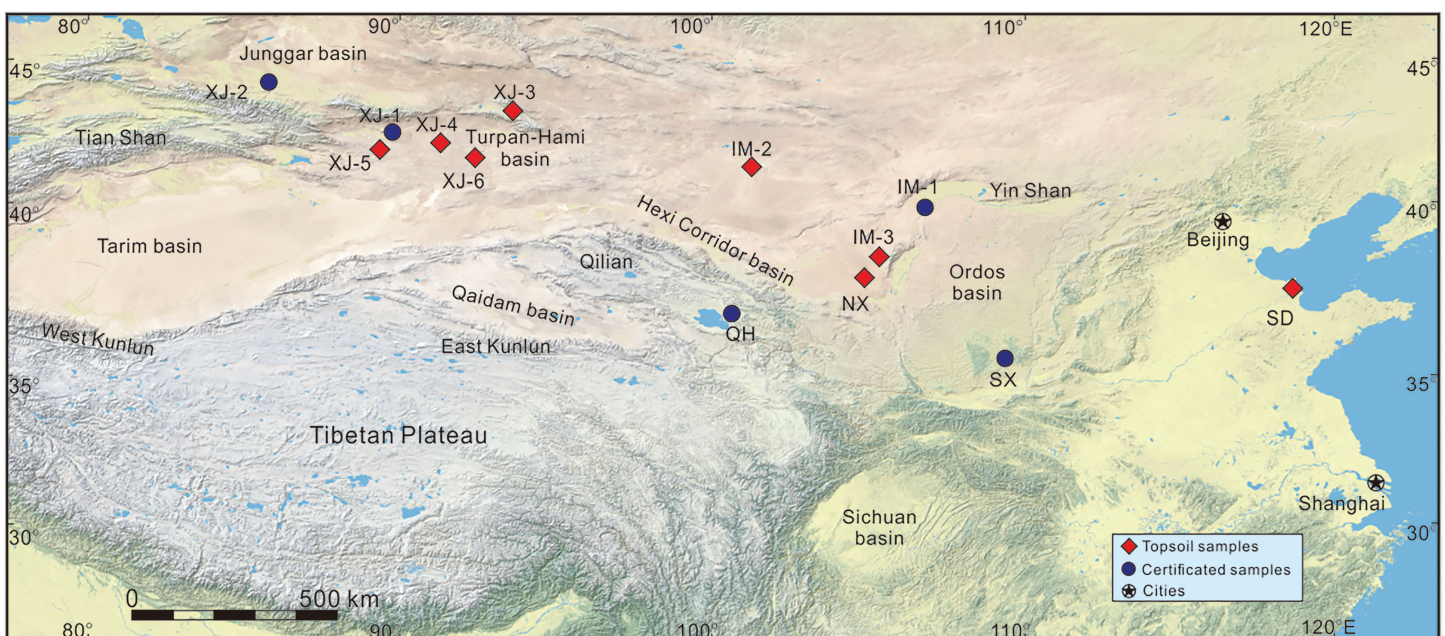


**Figure 1.** Geographical locations where samples used in this work were collected.

were stored in sealed plastic jars for further characterization. The five certificated samples have been processed by the supplier using a similar procedure, and therefore, they were used in our work without further pretreatment.

## 2.2. Sample Characterization

In this work we measured chemical and mineralogical compositions and hygroscopic properties of saline mineral dust samples, as described below.

### 2.2.1. Ion Chromatography Analysis

Around 20 mg soil powder was added into 20 mL ultrapure deionized water, and the mixture was stirred using an oscillating table for 2 hr. The solution was then filtered through a 0.2- $\mu\text{m}$  PTFE membrane syringe filter. Since ion concentrations were very high for some of the filtered solutions, those solutions were diluted by a factor of 10 or 100 before ion chromatography (IC) analysis if necessary. A Metrohm 761 Compact IC unit was employed in this work to analyze these solutions, and the analysis protocol could be found elsewhere (Fu et al., 2014). Five cations ( $\text{Na}^+$ ,  $\text{K}^+$ ,  $\text{Ca}^{2+}$ ,  $\text{Mg}^{2+}$ , and  $\text{NH}_4^+$ ) and seven anions ( $\text{F}^-$ ,  $\text{Br}^-$ ,  $\text{Cl}^-$ ,  $\text{NO}_2^-$ ,  $\text{NO}_3^-$ ,  $\text{PO}_4^{3-}$ , and  $\text{SO}_4^{2-}$ ) were analyzed. The detection limits were  $\sim 0.02$  mg/L for these ions, and  $\text{NH}_4^+$ ,  $\text{F}^-$ ,  $\text{Br}^-$ ,  $\text{NO}_2^-$ , and  $\text{PO}_4^{3-}$  were below detection limits for all the samples we examined.

### 2.2.2. X-ray Diffraction Analysis

X-ray diffraction (XRD) analysis was carried out using a Rigaku Ultima X-ray diffractometer with Cu K $\alpha$  radiation at 40 kV, 2 mA, and a wavelength of 1.54  $\text{\AA}$  (Jian et al., 2019). Approximately 1 g sample was deposited into the square trough (length: 20 mm, width: 16 mm, depth:  $\sim 0.9$  mm) in a cleaned glass slide, firmly pressed using another glass slide, and then transferred into the diffractometer. Scans were conducted for  $2\theta$  in the range of 5–65° with a resolution of 0.02° and a scanning speed of 4°/min, and thus, each scan took approximately 15 min. Data processing and mineral identification were performed using the MDI Jade software, and the K-value method was employed to convert the diffraction intensity to relative mass in a semiquantitative manner.

### 2.2.3. Hygroscopic Growth Measurements

Hygroscopic properties of saline mineral dust samples were investigated using a vapor sorption analyzer (Q5000SA), which measured mass change of a sample as a function of RH at a constant temperature using a highly sensitive balance. Measurements were all carried out at room temperature ( $25 \pm 0.1$  °C). Since instrumental and operational details can be found in our previous work (Gu et al., 2017; Guo et al., 2019; Tang et al., 2019), here we only provide a brief description of key features. The mass measurement range and sensitivity were 0–100 mg and 0.01  $\mu\text{g}$ , and the dry mass of samples examined in this work was in the range of 1–10 mg, depending on their hygroscopicity. The mass change of an empty sample holder was measured simultaneously to remove the background. The sample was housed in a temperature-regulated chamber, and one dry nitrogen flow and one humidified nitrogen flow, regulated using mass flow controllers, were mixed and then delivered into the chamber to control the RH (0–98%). The deliquescence of NaCl, KCl, and  $(\text{NH}_4)_2\text{SO}_4$  were routinely examined using this setup (Tang et al., 2019), and absolute differences were found to be <1% between the measured and theoretical deliquescence RH, suggesting that the accuracy in RH control could reach  $\pm 1\%$ .

For each experiment, as the first step, the sample was dried at <1% RH; RH was then increased to 90% RH, and at each step RH was increased by 10%; in the final, RH was returned to <1% to dry the sample again. Only when the sample was in equilibrium with the environment, RH was changed to the next value; at a given RH, the sample was considered to reach the equilibrium when its relative mass change was <0.05% within 30 min. Figure 2 displays the change of RH and sample mass (relative to that at <1% RH,  $m/m_0$ ) in two typical experiments. For each type of saline mineral dust examined in this work, at least three samples were measured, and the average relative mass changes (and the corresponding standard deviations) were reported.

## 2.3. Thermodynamic Calculations

One of the most widely used aerosol thermodynamic equilibrium models, ISORROPIA II (Fountoukis & Nenes, 2007), was employed to calculate mass growth factors at 90% RH for saline mineral dust samples examined in this work. A few other thermodynamic models are also available to predict aerosol hygroscopic growth (Clegg et al., 1998; Topping et al., 2005), and ISORROPIA II was chosen in our work because it is probably the most widely used one in the atmospheric chemistry community. Mass fractions of soluble

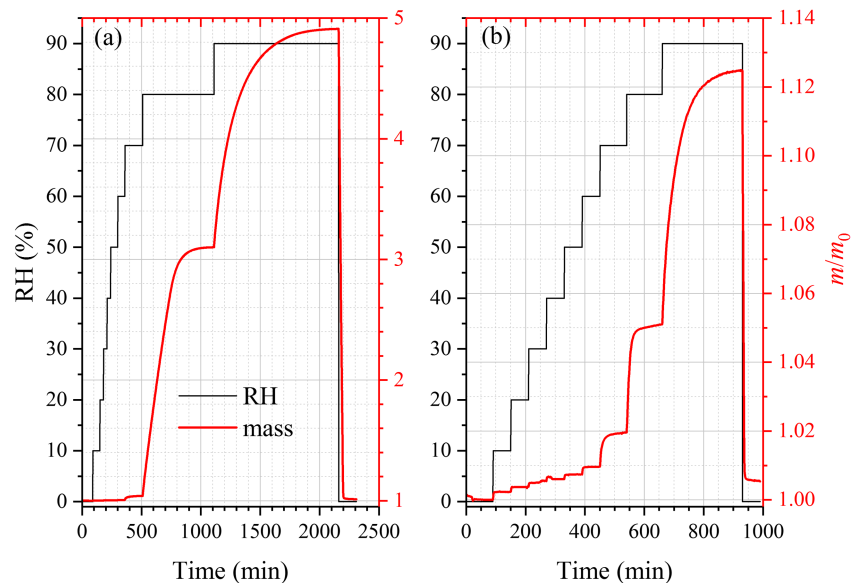


**Figure 2.** Time series of RH (left y axis, black curve) and  $m/m_0$  (sample mass relative to that at <1% RH, right y axis, red curve) in two typical experiments: (a) sample XJ-5 and (b) sample IM-1.

ions, which were derived from IC measurement, were used as model input. In our work the model was run at the “reverse” mode for which aerosol composition is known. For the “reverse mode,” we further run the model under both “stable” and “metastable” conditions, and the calculated mass growth factors at 90% RH were found to be identical under the two conditions. In addition, it was further assumed that the mass growth of other contents (e.g., quartz, feldspar, clay minerals) was negligible at 90% RH (Gaston et al., 2017; Tang et al., 2016); that is, hygroscopic growth of these samples were entirely attributed to soluble inorganic contents measured using IC.

### 3. Results and Discussion

#### 3.1. Mineralogical and Chemical Compositions

##### 3.1.1. Mineralogical Composition

XRD was used to measure mineralogical composition of saline mineral dust samples explored in this work, and in total 16 minerals have been identified. Figure 3 displays XRD spectra of XJ-1, XH-5, and IM-3, and the mass fractions of each mineral identified are summarized in Tables S1 and S2. As shown in Figure 3 and Tables S1 and S2, major minerals identified include quartz, orthoclase, albite, muscovite, and calcite, and these samples also contained significant amounts of clay minerals (e.g., kaolinite, chlorite, and illite) and Fe-containing minerals (e.g., hematite, goethite, and pyrite); in addition, aragonite, anhydrite, and rutile were identified in XJ-3, XJ-6, and IM-3, respectively. Mineralogical compositions of these samples were qualitatively consistent with those reported in literature for desert soils and mineral dust aerosols (Engelbrecht et al., 2016; Formenti et al., 2014; Ito & Wagai, 2017; Journet et al., 2014; Shi et al., 2005), as similar minerals have been identified in our work and these studies.

More importantly, XRD analysis revealed the presence of two highly soluble minerals, that is, thenardite ( $\text{Na}_2\text{SO}_4$ ) and halite ( $\text{NaCl}$ ), in some of the samples investigated. While thenardite was identified only in one sample (IM-3), halite was identified in eight (XJ-1, XJ-3, XJ-4, XJ-5, XJ-6, IM-2, NX, and SD) of the 13 samples studied in this work. At around room temperature,  $\text{NaCl}$  and  $\text{Na}_2\text{SO}_4$  would deliquesce at ~75% and ~85% RH (Martin, 2000), respectively. Once deliquesced, the mass of  $\text{NaCl}$  and  $\text{Na}_2\text{SO}_4$  would be substantially increased due to water uptake. The presence of halite and thenardite in these samples would have important implications for their hygroscopic properties, as further discussed in section 3.2.

##### 3.1.2. Chemical Composition

Ion chromatography was employed to analyze water-soluble inorganic ions contained by saline mineral dust samples investigated in this work, and the results are summarized in Table 2. The presence of  $\text{NH}_4^+$ ,  $\text{F}^-$ ,  $\text{Br}^-$ ,

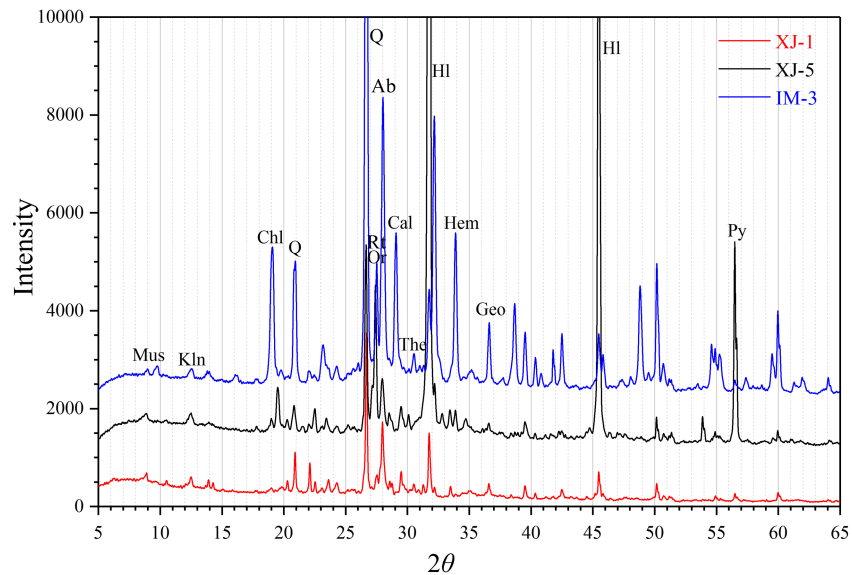


**Figure 3.** XRD spectra of XJ-1, XJ-5, and IM-3 samples. Ab = albite (3.21 Å), Cal = calcite (3.04 Å), Chl = chlorite (4.74 Å), Goe = goethite (2.46 Å), Hem = hematite (2.71 Å), HI = halite (2.00 Å), Kln = kaolinite (7.25 Å), Mus = muscovite (9.89 Å), Or = orthoclase (3.26 Å), Py = pyrite (1.63 Å), Q = quartz (3.34 Å), Rt = rutile (3.24 Å), The = thenardite (2.78 Å).

$\text{NO}_2^-$ , and  $\text{PO}_4^{3-}$  were negligible for all the samples, and only small amount of  $\text{NO}_3^-$  was detected in a few samples (i.e., XJ-1, XJ-4, and XJ-5) with mass fractions found to be  $<0.3\%$ . As shown in Table 2, the mass fractions of soluble inorganic ions measured varied by more than 2 orders of magnitude, ranging from  $<0.5\%$  (i.e., XJ-2 and SX) to  $>84\%$  (NX). Among the four cations identified,  $\text{Na}^+$  was usually the most abundant one, and the contribution of  $\text{Ca}^{2+}$  and  $\text{Mg}^{2+}$  could be significant and even dominant for a few samples, while  $\text{K}^+$  was minor. For anions,  $\text{Cl}^-$  and  $\text{SO}_4^{2-}$  were the two major components, and their relative contributions were highly variable. Gaston et al. (2017) analyzed 10 saline mineral dust samples collected in North America, and found that cations were mainly contributed by  $\text{Na}^+$  or  $\text{Mg}^{2+}$  while anions were mainly contributed by  $\text{Cl}^-$  or  $\text{SO}_4^{2-}$ . The chemical compositions of saline mineral dust in North America were qualitatively similar to those in China.

### 3.2. Hygroscopic Properties

Mass changes were measured as a function of RH (up to 90%) for all the 13 saline mineral dust samples. Tables S3–S5 compile mass growth factors at different RH (defined as the mass ratio at a given RH to that

at  $<1\%$  RH) for all the samples, and their mass growth factors at 90% RH are shown in Table 3. Large variations in hygroscopic properties were observed for the samples investigated, and their mass growth factors at 90% RH ranged from  $\sim 1.02$  (SX) to  $\sim 6.7$  (NX); in other words, the mass increase at 90% RH, when compared to that at  $<1\%$  RH, increased from only  $\sim 2\%$  to as large as  $\sim 5.7$ . For comparison, the mass growth factors are 7.29 and 3.49 for NaCl and  $\text{Na}_2\text{SO}_4$  at 90% RH, respectively (Clegg et al., 1998). A quartz crystal balance was used to investigate mass change of China loess at different RH (Navea et al., 2010), and the sample mass was increased by  $>15\%$  when RH increased from  $<1\%$  to 70%. In our work one China loess sample (the sample name is SX) was also studied, and as shown in Table S5, when RH was increased from  $<1\%$  to 70%, the sample mass was only increased by  $\sim 1.2\%$ , significantly smaller than that reported by Navea et al. (2010). China loess samples used in these two studies may have different chemical composition, and if so their hygroscopicity would differ; however, chemical composition of the China loess sample used by Navea et al. (2010) was not reported, making it

**Table 2**  
Mass Fractions (%) of Soluble Ions for Different Mineral Dust Samples Examined in This Work

Sample	$\text{Na}^+$	$\text{K}^+$	$\text{Ca}^{2+}$	$\text{Mg}^{2+}$	$\text{NO}_3^-$	$\text{Cl}^-$	$\text{SO}_4^{2-}$	Total
XJ-1	4.47	0.10	0.02	1.18	0.21	2.96	12.08	21.01
XJ-2	0.07	0.05	0.03	0.33	n. d.	0.00	0.02	0.49
XJ-3	2.39	0.05	0.04	0.45	n. d.	0.93	4.97	8.83
XJ-4	3.26	0.02	0.02	0.33	0.21	3.41	0.71	7.96
XJ-5	24.07	0.04	0.48	0.55	0.29	21.45	9.73	56.62
XJ-6	0.03	0.01	0.11	6.51	n. d.	0.00	34.11	40.77
IM-1	0.76	0.05	0.04	0.44	n. d.	0.56	2.12	3.96
IM-2	4.71	0.10	0.72	0.81	n. d.	2.29	14.13	22.77
IM-3	13.43	0.04	0.04	0.92	n. d.	0.95	34.24	49.61
QH	0.06	0.05	0.04	0.40	n. d.	0.02	0.21	0.77
NX	35.37	0.15	0.34	0.06	n. d.	38.70	9.58	84.21
SX	0.03	0.04	0.03	0.35	n. d.	n. d.	n. d.	0.45
SD	2.65	0.03	0.41	1.90	n. d.	5.08	7.54	17.61

Note. n.d. = not detected.

**Table 3**  
Mass Growth Factors at 90% RH and Single Hygroscopicity Parameters ( $\kappa$ ) of Saline Mineral Dust Samples Investigated in This Work

Sample	Hygroscopicity	MGF <sub>m</sub>	MGF <sub>c</sub>	MGF <sub>c</sub> /MGF <sub>m</sub>	$\kappa$
XJ-1	M <sup>a</sup>	1.6569 ± 0.0053	1.415	0.85	0.190
XJ-2	L <sup>a</sup>	1.0312 ± 0.0001	1.000	0.97	0.009
XJ-3	L	1.2602 ± 0.0030	1.256	1.00	0.075
XJ-4	M	1.7183 ± 0.0071	1.410	0.82	0.207
XJ-5	H <sup>a</sup>	4.9258 ± 0.0139	3.390	0.69	1.134
XJ-6	L	1.1212 ± 0.0048	2.208	1.97	0.035
IM-1	L	1.1237 ± 0.0008	1.121	1.00	0.036
IM-2	M	1.7353 ± 0.0165	1.428	0.82	0.212
IM-3	M	1.9732 ± 0.0200	2.313	1.17	0.281
QH	L	1.0215 ± 0.0001	1.007	0.99	0.006
NX	H	6.7060 ± 0.0227	5.064	0.76	1.648
SX	L	1.0212 ± 0.0003	1.000	0.98	0.006
SD	M	1.7910 ± 0.0471	1.624	0.91	0.229

Note. MGF<sub>m</sub> = measured mass growth factors at 90% RH, MGF<sub>c</sub> = calculated mass growth factors at 90% RH.  
<sup>a</sup>According to their hygroscopicity, samples examined in this work were broadly classified into three catalogues (L = low hygroscopicity, M = medium hygroscopicity, H = high hygroscopicity).

difficult to assess if the difference in measured hygroscopicity can be fully attributed to the difference in chemical composition.

### 3.2.1. Effect of Mineralogical Composition

According to their hygroscopicity, the 13 samples examined in this work could be broadly classified into three catalogues. Six samples, including XJ-2, XJ-3, XJ-6, IM-1, QH, and SX, belonged to the low-hygroscopicity group, and their mass growth factors at 90% RH were ~1.03 or smaller. As shown in Tables S1 and S2, no halite or thenardite was identified by XRD for XJ-2, IM-1, QH, and SX, and all the four samples fell into the low-hygroscopicity group, indicating that the presence of halite or thenardite, which were both highly water-soluble minerals, played important roles in determining the hygroscopic properties of saline mineral dust. The medium-hygroscopicity group contained five samples (XJ-1, XJ-4, IM-2, IM-5, and SD), and their mass growth factors at 90% RH were in the range of 1.6–2.0. The high-hygroscopicity group had two samples (XJ-5 and NX), with mass growth factors being ~4.9 and ~6.7 at 90% RH, respectively. Saline mineral dust samples with medium and high hygroscopicity all contained substantial amount of halite or thenardite, as Tables S1 and S2 suggested.

Figure 4 shows mass growth factors as a function of RH for six samples, and comprehensive information of mass growth factors at different RH can be found in Tables S3–S6 for all the samples studied. For most of the samples with medium or high hygroscopicity, significant mass growth occurred when RH was increased to 80% RH, and the corresponding mass growth factors were found to be >1.26 at 80% RH. This could be explained by dominance of halite (NaCl) in the soluble minerals for these samples: NaCl would deliquesce when RH exceeded its deliquescence RH (~75%), leading to significant increase in sample mass. The only exception was IM-3, for which mass growth factors were measured to be ~1.97 at 90% RH and ~1.14 at 80% RH, as shown in Figure 4 and Table S4; for comparison, the mass growth factors were 1.71–1.74 (smaller than IM-3) at 90% RH and 1.33–1.39 (larger than IM-3) at 80% RH. As discussed in section 3.1.1, XRD analysis suggested that IM-3 was the only sample which contained significant amount of thenardite (Na<sub>2</sub>SO<sub>4</sub>), which would deliquesce at ~85% RH. As a result, when RH was increased from 70% to 80%, relative mass increase was not as profound for IM-3 as other samples with medium or high hygroscopicity.

It could be further concluded from data compiled in Tables S3–S5 that SD was the only sample whose mass growth factor reached 1.16 at 70% RH, and at the same RH the mass growth factors were smaller than 1.04 for all the other samples. In fact, SD exhibited significant and continuous growth even at lower RH: for example, its mass growth factors were found to be ~1.03 and ~1.08 at 30% and 60%, respectively. This is because SD contained similar amount of soluble magnesium and sodium ions, and magnesium salts (e.g., MgCl<sub>2</sub>) would deliquesce at considerably lower RH (Cziczo & Abbatt, 2000; Guo et al., 2019; Gupta et al., 2015). As magnesium salts might exist in amorphous states, they were not detected via XRD.

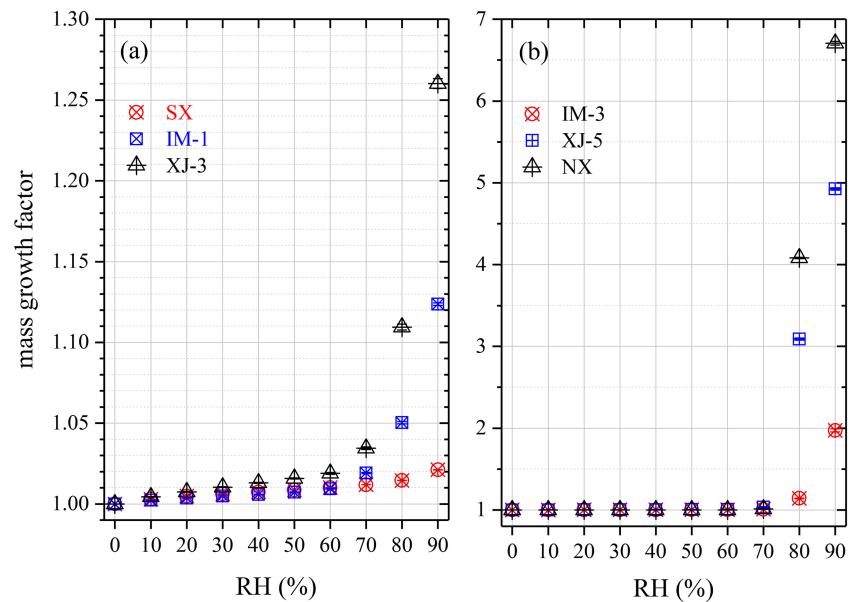


**Figure 4.** Measured mass growth factors of six different saline mineral dust samples as a function of RH. (a) SX, IM-1, and XJ-3 and (b) IM-3, XJ-5, and NX.

However, a more quantitative relation between hygroscopic properties and mineralogical composition could be not obtained. For example, Table S1 shows that the mass fraction of halite was 14% for XJ-6, larger than that for XJ-4; however, as displayed in Table 3, the mass growth factor at 90% RH was  $\sim 1.12$  for XJ-6, significantly smaller than that for XJ-4 ( $\sim 1.72$ ). The main reason is that XRD could only detect well-crystallized minerals (Nowak et al., 2018), and unidentified materials, some of which may be highly hygroscopic, could be substantial. Furthermore, XRD analysis is at most a semiquantitative method, and therefore, the derived mass fractions should be used with caution. As a result, in section 3.2.2 we further sought to explain the measured mass growth factors using mass fractions of soluble ions determined using IC.

### 3.2.2. Effect of Soluble Ions

The relationship between hygroscopic properties of saline mineral dust samples and their chemical compositions was explored. The dependence of mass growth factors at 90% RH on mass fractions of  $\text{Na}^+$  was plotted in Figure 5a, revealing a good correlation ( $R^2 = 0.957$ ) between hygroscopic properties and mass fractions of  $\text{Na}^+$ ; a similar correlation ( $R^2 = 0.943$ ) was found to exist between mass growth factors at 90% RH and the total mass fractions of all the cations (i.e.,  $[\text{Na}^+] + [\text{K}^+] + [\text{Ca}^{2+}] + [\text{Mg}^{2+}]$ ), as shown in Figure 5b. This is understandable since  $\text{Na}^+$  was usually the major cation for saline mineral dust samples examined in this work. Similarly, a good correlation ( $R^2 = 0.974$ ) between mass growth factors at 90% RH and mass fractions of  $\text{Cl}^-$  was found; for comparison, mass growth factors were well correlated with the sum of mass fractions of  $\text{Cl}^-$  and  $\text{SO}_4^{2-}$ , if the two samples, XJ-6 and IM-3, were excluded from analysis. The reason may be that  $\text{SO}_4^{2-}$  were overwhelmingly dominated over  $\text{Cl}^-$  for both XJ-6 and IM-3.

Overall, Figures 5 and 6 suggested in a qualitative manner that chemical composition played a key role in hygroscopic properties of saline mineral dust. Similar conclusions were drawn by Gaston et al. (2017) for saline mineral dust in North America, who found good correlations between CCN activities and aerosol composition measured using aerosol time-of-flight mass spectrometry.

### 3.3. Discussion

To further explore the dependence of hygroscopic properties of saline mineral dust samples on their chemical composition, mass fractions of soluble ions (shown in Table 2) were used as input in the ISORROPIA-II model to calculate mass growth factors at 90% RH, and the calculated mass growth factors were then compared with the measured values. The measured and calculated mass growth factors at 90% RH, as well as their ratios, are summarized in Table 3 for the 13 samples investigated, and Figure 7 displays the comparison between measured and calculated mass growth factors. As shown in Table 3 and Figure 7, the difference

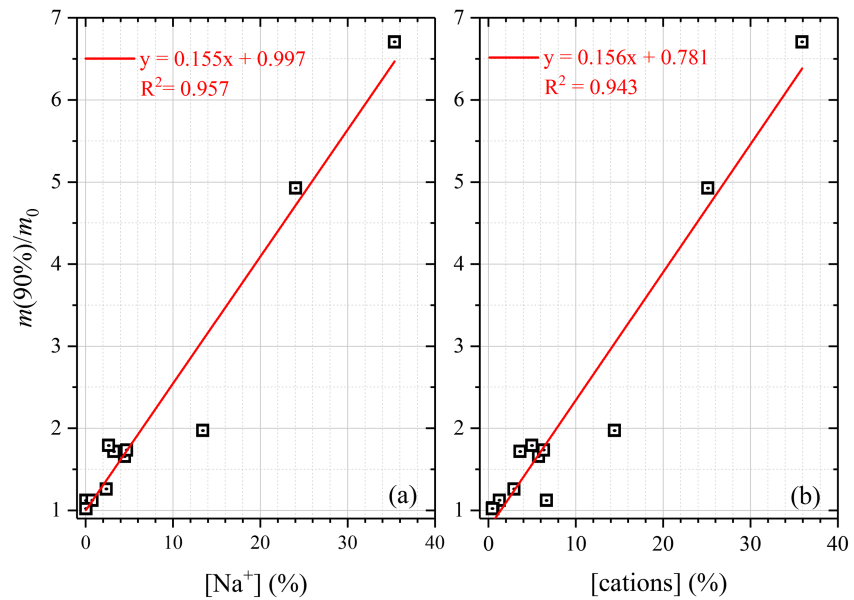


**Figure 5.** Dependence of measured mass growth factors at 90% RH on mass fractions of (a)  $\text{Na}^+$  and (b) total cations.

between measured and calculated mass growth factors was found to be <20%, except XJ-5, XJ-6, and NX, suggesting that overall ISORROPIA-II performed reasonably well in predicting hygroscopic properties of saline mineral dust samples. The calculated mass factors at 90% RH were 31% and 24% smaller than the measured values for XJ-5 and NX, respectively; in contrast, for XJ-6, the calculated mass growth factor at 90% RH was 97% larger than the measured value.

Gaston et al. (2017) used ISORROPIA-II to predict  $\kappa$  values for saline mineral dust samples collected in North America, and compared predicted values with those derived from CCN activity measurements. Fairly good agreement between prediction and measurement was found for most of the sample, although large discrepancies also existed for a few samples (Gaston et al., 2017). For example, the measured  $\kappa$  was

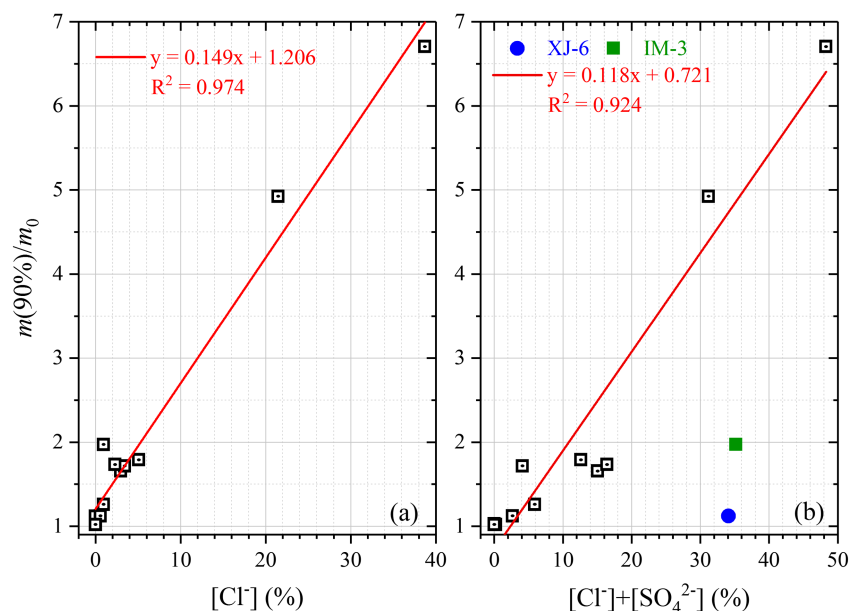


**Figure 6.** Dependence of measured mass growth factors at 90% RH on mass fractions of (a)  $\text{Cl}^-$  and (b)  $\text{Cl}^-$  plus  $\text{SO}_4^{2-}$  (XJ-6 and IM-3 were excluded from correlation analysis).

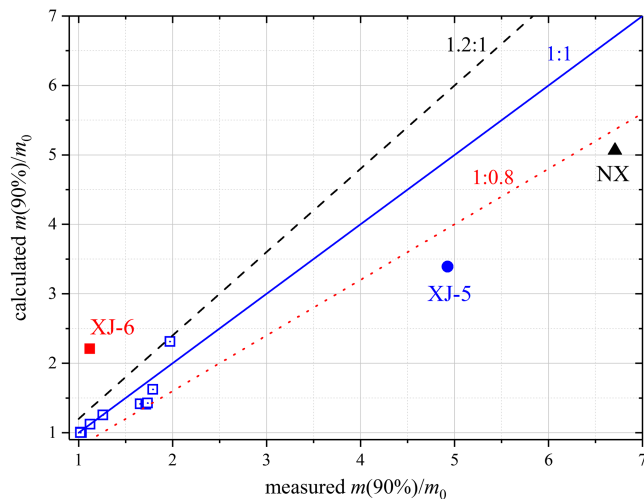


**Figure 7.** Comparison between measured mass growth factors at 90% RH ( $m(90\%)/m_0$ ) and those calculated using ISORROPIA-II. The three lines are 1.2:1 (dashed black), 1:1 (solid blue), and 1:0.8 (dotted red) lines.

$0.052 \pm 0.004$  for one sample (TX Salt Basin Site S3), significantly larger than the predicted value (0.001); on the other hand,  $\kappa$  were measured to be  $0.041 \pm 0.006$  and  $0.033 \pm 0.004$  for another two samples (Great Salt Lake “Puffy Soil” and Great Salt Lake “Salt Crust”), approximately 1 order of magnitude smaller than corresponding predicted values (0.374 and 0.348, respectively). Overall, the agreement between measurement and calculation appeared to be better in our present work, when compared to the study by Gaston et al. (2017). Both studies used the bulk average chemical composition, measured using IC, as input for thermodynamic calculations; however, our work measured hygroscopic growth of bulk samples, whereas Gaston et al. (2017) measured the CCN activities of aerosol particles, the chemical composition of which may be different from those for the bulk samples. Therefore, better agreement between measured and predicted hygroscopicity could be expected for our study, when compared to the work by Gaston et al. (2017).

### 3.4. Atmospheric Implications

#### 3.4.1. Implications for Heterogeneous Chemistry

A number of studies (Krueger et al., 2004; Laskin et al., 2005; Li et al., 2014; Rubasinghege & Grassian, 2013; Tang et al., 2014) have revealed the important roles chemical composition of mineral dust and its hygroscopicity play in heterogeneous reactions of mineral dust with various trace gases. It is conventionally believed that fresh mineral dust particles mainly consist of low-hygroscopicity minerals, and our work found that saline mineral dust particles could contain substantial amounts of soluble materials and thus exhibit considerable hygroscopicity, and therefore display different heterogeneous reactivity when compared to “conventional” mineral dust. For example, a very recent study (Mitroo et al., 2019) explored heterogeneous reaction of  $N_2O_5$  with saline mineral dust particles collected from different regions in North America. Significant production of  $ClNO_2$ , in addition to  $N_2O_5$  uptake, was observed, indicating that saline mineral dust particles could be an important source for chlorine species (e.g.,  $ClNO_2$ ) in continental North America (Mitroo et al., 2019). Our present work showed that the amounts of chloride could be substantial for saline mineral dust particles collected in northern China, where high levels of  $N_2O_5$  up to several parts per billion by volume were observed (Wang et al., 2017; Wang et al., 2018; Zhou et al., 2018). Therefore, heterogeneous reactions of saline mineral dust particles can be an important source for the observed  $ClNO_2$  in north China. In addition to airborne saline mineral dust particles, dry deposition of  $N_2O_5$  to saline topsoil may also contribute to  $N_2O_5$  removal and  $ClNO_2$  production, although its effects remain to be assessed.

Aerosol liquid water (or surface-adsorbed water) largely determines kinetics, mechanisms, and products of heterogeneous reactions (Rubasinghege & Grassian, 2013; Tang et al., 2017; Wu et al., 2018). Mitroo et al. (2019) found that at a given RH,  $N_2O_5$  uptake coefficients decreased whereas  $ClNO_2$  production yield increased with soluble ion fractions in saline mineral dust samples. Furthermore, the dependence of  $N_2O_5$  uptake coefficients on RH was found to vary with different samples in complicated manners, indicating competing effects between uptake by clay minerals and uptake by soluble contents. Experiment work are ongoing to determine the dependence of  $N_2O_5$  uptake coefficients and  $ClNO_2$  yields on RH for heterogeneous interactions of  $N_2O_5$  with saline mineral dust samples examined herein. Chemical composition and hygroscopic properties of saline mineral dust particles, as measured in our work, would help better understand and predict their heterogeneous reactions with  $N_2O_5$  and other reactive trace gases as well.

#### 3.4.2. Implications for Cloud Condensation Nucleation

When the Kelvin effect is negligible,  $\kappa$  can be determined from particle volumes under dry and humidified conditions using equations (1) and (2):

$$RH = \frac{V/V_0 - 1}{V/V_0 - (1 - \kappa)} \quad (1)$$

$$\kappa = \left( \frac{V}{V_0} - 1 \right) \frac{1 - RH}{RH} \quad (2)$$

where  $V_0$  is the particle volume at dry conditions and  $V$  is the particle volume at a given RH. In this work hygroscopic properties measured at 90% RH were used to derive  $\kappa$  values. If we assume that particle volume at a given RH is equal to the sum of particle volume at dry conditions and the volume of particulate water at a given RH ( $V_w$ ), equation (3) can then be derived:

$$\frac{V}{V_0} = 1 + \frac{V_w}{V_0} = 1 + \frac{m_w/\rho_w}{m_0/\rho_0} = 1 + \frac{m_w}{m_0} \cdot \frac{\rho_0}{\rho_w} \quad (3)$$

where  $m_0$  and  $m_w$  are the dry particle mass and the mass particulate water and  $\rho_0$  and  $\rho_w$  are the densities of the dry particle and water, respectively. In addition to insoluble components, NaCl and Na<sub>2</sub>SO<sub>4</sub> were found to be the major components for saline mineral dust samples examined in this work. The densities are 2.16, 2.68, and 2.6–2.9 g/cm<sup>3</sup> for NaCl, Na<sub>2</sub>SO<sub>4</sub>, and authentic desert dust samples (as well as common insoluble minerals they contain; Tang et al., 2014; Tang et al., 2012; Wagner et al., 2009), and in the present work the density was assumed to be 2.6 g/cm<sup>3</sup> for saline mineral dust samples under dry conditions. As a result, volume changes and consequently  $\kappa$  values could then be derived from measured mass changes at 90% RH relative to that at dry conditions, using equation (3) and then equation (2). The derived  $\kappa$  values are displayed in Table 3, spanning from <0.01 (for XJ-2, QH and SX) to >1.1 (1.134 for XJ-5 and 1.648 for NX). The  $\kappa$  values may be overestimated for XJ-5 and NX, as NaCl was the dominant component for these two samples, and thus, their densities should be close to that for NaCl (2.16 g/cm<sup>3</sup>). If their densities were assumed to be equal to that for NaCl, the  $\kappa$  values were calculated to be 0.942 and 1.369 for XJ-5 and NX, respectively.

Hygroscopicity and CCN activity of mineral dust aerosol are conventionally thought to be rather limited ( $\kappa < 0.01$ ; Herich et al., 2009; Koehler et al., 2009; Tang et al., 2016). Nevertheless, field measurements suggested that saline mineral dust particles played a significant role in cloud droplet formation over the North American continent (Pratt et al., 2010). This observation was further supported by laboratory studies which showed that saline mineral dust particles in North America exhibited considerably high hygroscopicity and CCN activity (Gaston et al., 2017; Koehler et al., 2007). For example,  $\kappa$  values were measured to be in the range of <0.01 to >0.8 for saline mineral dust particles collected in North America (Gaston et al., 2017), displaying large geographical variations. In our work we measured hygroscopic growth of saline mineral dust particles in China, and also found that the derived  $\kappa$  values varied from <0.01 to >1. Therefore, our work provided experimental data to support the idea that saline mineral dust particles could be important for cloud droplet formation, and their hygroscopicity depended on chemical composition and thus may vary largely with geographical locations.

It should be pointed out that the average chemical composition and hygroscopic properties were measured in our work for these samples, and thus, average  $\kappa$  values were derived. In addition to the average composition of aerosol particles, mixing state is known to be important in determining hygroscopic properties and CCN activity of individual particles, and it would make a difference whether soluble materials contained by a saline mineral dust sample are only distributed in some individual particles or internally mixed with nonsoluble minerals. Single particle technique (Chi et al., 2015; Li et al., 2014) can be very valuable to understand the mixing state of individual saline mineral dust particles and their hygroscopicity.

#### 4. Conclusion

It has been suggested that saline mineral dust aerosol particles, which occur in various locations over the globe, play important roles in the troposphere. They could contribute largely to the observed mass concentration of particulate matter, participate in cloud droplet formation, and be an important source of reactive chlorine species over continental regions. However, hygroscopicity of saline mineral dust particles, especially for those found in regions other than North America, remains to be elucidated.

In this work we measured their relative mass change as a function of RH (up to 90%) to investigate hygroscopic properties of 13 saline mineral dust samples originating from different locations in north China, which is a globally important mineral dust source region. In addition, their chemical and mineralogical compositions were analyzed using ion chromatography and X-ray diffraction. The mass growth factors (sample mass relative to that at <1% RH) were measured to span from ~1.02 to 6.7 at 90% RH, displaying large geographical variation, and the corresponding single hygroscopicity parameters ( $\kappa$ ) were derived to be in the range of <0.01 to >1.0. XRD analysis suggested that many saline mineral dust samples contained

thenardite ( $\text{Na}_2\text{SO}_4$ ) and halite ( $\text{NaCl}$ ), which were soluble minerals and contributed to the observed hygroscopic growth of these samples. It was further found that hygroscopic properties of saline mineral dust samples examined largely depended on the mass fractions of soluble ions, which were mainly  $\text{Na}^+$ ,  $\text{Cl}^-$ , and  $\text{SO}_4^{2-}$ . The mass fractions of soluble ions were used as input in the ISORROPIA model to calculate mass growth factors at 90% RH, and the calculated growth factors were found to agree with measured values within 20% for 10 of the 13 samples. For the other three samples, both overestimation and underestimation of calculations, when compared to measurements, were observed. Overall, this work would significantly improve our knowledge of composition and hygroscopic properties of saline mineral dust particles, helping better understand their environmental and climatic impacts via heterogeneous reactions and cloud droplet formation.

### Competing Interests

The authors declare that they have no conflict of interest.

### Author's Contribution

Mingjin Tang designed the research (with input from Binqi Zhu, Luhua Xie, Zhe Wang, and Xinming Wang), analyzed the data, and wrote the manuscript with contributions from all the coauthors; Huanhuan Zhang, Wenjun Gu, Liya Guo, and Xiaoyan Gao conducted experimental work with supervision by Mingjin Tang, Xing Jian, Guohua Zhang, and Xinming Wang; and Jie Gao and Guoliang Shi performed the thermodynamic calculation and interpreted the data.

### Acknowledgments

This work was funded by National Natural Science Foundation of China (91744204, 91644106, and 41673009), Chinese Academy of Sciences (132744KYSB20160036), State Key Laboratory of Organic Geochemistry (SKLOG2016-A05), and Guangdong Foundation for Program of Science and Technology Research (2017B030314057). Mingjin Tang would like to thank the CAS Pioneer Hundred Talents program for providing a starting grant. This is contribution IS-2747 from GIGCAS. Data supporting this paper can be found at <http://doi.org/10.5281/zenodo.3359320>.

### References

- Abuduwaali, J., Gabchenko, M. V., & Junrong, X. (2008). Eolian transport of salts—A case study in the area of Lake Ebinur (Xinjiang, northwest China). *Journal of Arid Environments*, *72*, 1843–1852.
- Abuduwaali, J., Liu, D. W., & Wu, G. Y. (2010). Saline dust storms and their ecological impacts in arid regions. *Journal of Arid Land*, *2*, 144–150.
- Balkanski, Y., Schulz, M., Claquin, T., & Guibert, S. (2007). Reevaluation of mineral aerosol radiative forcings suggests a better agreement with satellite and AERONET data. *Atmospheric Chemistry and Physics*, *7*, 81–95.
- Blank, R. R., Young, J. A., & Allen, F. L. (1999). Aeolian dust in a saline playa environment, Nevada, USA. *Journal of Arid Environments*, *41*, 365–381.
- Bucher, E. H., & Stein, A. F. (2016). Large salt dust storms follow a 30-year rainfall cycle in the Mar Chiquita Lake (Cordoba, Argentina). *PLoS ONE*, *11*.
- Chen, S. Y., Huang, J. P., Kang, L. T., Wang, H., Ma, X. J., He, Y. L., et al. (2017). Emission, transport, and radiative effects of mineral dust from the Taklimakan and Gobi deserts: Comparison of measurements and model results. *Atmospheric Chemistry and Physics*, *17*, 2401–2421.
- Chi, J. W., Li, W. J., Zhang, D. Z., Zhang, J. C., Lin, Y. T., Shen, X. J., et al. (2015). Sea salt aerosols as a reactive surface for inorganic and organic acidic gases in the Arctic troposphere. *Atmospheric Chemistry and Physics*, *15*, 11,341–11,353.
- Clegg, S. L., Brimblecombe, P., & Wexler, A. S. (1998). Thermodynamic model of the system  $\text{H}^+ - \text{NH}_4^+ - \text{Na}^+ - \text{SO}_4^{2-} - \text{NO}_3^- - \text{Cl}^- - \text{H}_2\text{O}$  at 298.15 K. *The Journal of Physical Chemistry. A*, *102*, 2155–2171.
- Conway, T. M., & John, S. G. (2014). Quantification of dissolved iron sources to the North Atlantic Ocean. *Nature*, *511*, 212–215.
- Creamean, J. M., Suski, K. J., Rosenfeld, D., Cazorla, A., DeMott, P. J., Sullivan, R. C., et al. (2013). Dust and biological aerosols from the Sahara and Asia influence precipitation in the western US. *Science*, *339*, 1572–1578.
- Cziczo, D. J., & Abbatt, J. P. D. (2000). Infrared observations of the response of  $\text{NaCl}$ ,  $\text{MgCl}_2$ ,  $\text{NH}_4\text{HSO}_4$ , and  $\text{NH}_4\text{NO}_3$  aerosols to changes in relative humidity from 298 to 238 K. *The Journal of Physical Chemistry. A*, *104*, 2038–2047.
- Cziczo, D. J., Froyd, K. D., Hoose, C., Jensen, E. J., Diao, M., Zondlo, M. A., et al. (2013). Clarifying the dominant sources and mechanisms of cirrus cloud formation. *Science*, *340*, 1320–1324.
- Di Biagio, C., Formenti, P., Balkanski, Y., Caponi, L., Cazaunau, M., Pangui, E., et al. (2017). Global scale variability of the mineral dust long-wave refractive index: A new dataset of in situ measurements for climate modeling and remote sensing. *Atmospheric Chemistry and Physics*, *17*, 1901–1929.
- Dupart, Y., King, S. M., Nekat, B., Nowak, A., Wiedensohler, A., Herrmann, H., et al. (2012). Mineral dust photochemistry induces nucleation events in the presence of  $\text{SO}_2$ . *Proceedings of the National Academy of Sciences of the United States of America*, *409*, 20,842–20,847.
- Engelbrecht, J. P., Moosmüller, H., Pinnock, S., Jayanty, R. K. M., Lersch, T., & Casuccio, G. (2016). Technical note: Mineralogical, chemical, morphological, and optical interrelationships of mineral dust re-suspensions. *Atmospheric Chemistry and Physics*, *16*, 10,809–10,830.
- Formenti, P., Caquineau, S., Desboeufs, K., Klaver, A., Chevaillier, S., Journet, E., & Rajot, J. L. (2014). Mapping the physico-chemical properties of mineral dust in western Africa: Mineralogical composition. *Atmospheric Chemistry and Physics*, *14*, 10,663–10,686.
- Formenti, P., Elbert, W., Maenhaut, W., Haywood, J., & Andreae, M. O. (2003). Chemical composition of mineral dust aerosol during the Saharan Dust Experiment (SHADE) airborne campaign in the Cape Verde region, September 2000. *Journal of Geophysical Research*, *108*(18), 8576. <https://doi.org/10.1029/2002JD002648>
- Formenti, P., Schutz, L., Balkanski, Y., Desboeufs, K., Ebert, M., Kandler, K., et al. (2011). Recent progress in understanding physical and chemical properties of African and Asian mineral dust. *Atmospheric Chemistry and Physics*, *11*, 8231–8256.

- Fountoukis, C., & Nenes, A. (2007). ISORROPIA II: A computationally efficient thermodynamic equilibrium model for  $K^+$ - $Ca^{2+}$ - $Mg^{2+}$ - $NH_4^+$ - $Na^+$ - $SO_4^{2-}$ - $NO_3^-$ - $Cl^-$ - $H_2O$  aerosols. *Atmospheric Chemistry and Physics*, 7, 4639–4659.
- Frie, A. L., Dingle, J. H., Ying, S. C., & Bahreini, R. (2017). The effect of a receding saline lake (The Salton Sea) on airborne particulate matter composition. *Environmental Science & Technology*, 51, 8283–8292.
- Fu, X. X., Wang, X. M., Guo, H., Cheung, K., Ding, X., Zhao, X., et al. (2014). Trends of ambient fine particles and major chemical components in the Pearl River Delta region: Observation at a regional background site in fall and winter. *Science of the Total Environment*, 497, 274–281.
- Gaston, C. J., Pratt, K. A., Suski, K. J., May, N. W., Gill, T. E., & Prather, K. A. (2017). Laboratory studies of the cloud droplet activation properties and corresponding chemistry of saline playa dust. *Environmental Science & Technology*, 51, 1348–1356.
- Gholamipour, A., Nabizadeh, R., Hassanvand, M. S., Taghipour, H., Nazmara, S., & Mahvi, A. H. (2015). Characterization of saline dust emission resulted from Urmia Lake drying. *Journal of Environmental Health Science and Engineering*, 13, 82. <https://doi.org/10.1186/s40201-40015-40238-40203>
- Gill, T. E. (1996). Eolian sediments generated by anthropogenic disturbance of playas: Human impacts on the geomorphic system and geomorphic impacts on the human system. *Geomorphology*, 17, 207–228.
- Gillette, D. A., Stensland, G. J., Williams, A. L., Barnard, W., Gatz, D., Sinclair, P. C., & Johnson, T. C. (1992). Emissions of alkaline elements calcium, magnesium, potassium, and sodium from open sources in the contiguous United States. *Global Biogeochemical Cycles*, 6, 437–457.
- Ginoux, P., Prospero, J. M., Gill, T. E., Hsu, N. C., & Zhao, M. (2012). Global-scale attribution of anthropogenic and natural dust sources and their emission rates based on MODIS deep blue aerosol products. *Reviews of Geophysics*, 50, RG3005. <https://doi.org/10.1029/2012RG000388>
- Gu, W. J., Li, Y., Zhu, J., Jia, X., Lin, Q., Zhang, G., et al. (2017). Investigation of water adsorption and hygroscopicity of atmospherically relevant particles using a commercial vapor sorption analyzer. *Atmospheric Measurement Techniques*, 10, 3821–3832.
- Guo, L. Y., Gu, W. J., Peng, C., Wang, W. G., Li, Y. J., Zong, T. M., et al. (2019). A comprehensive study of hygroscopic properties of calcium and magnesium-containing salts: Implication for hygroscopicity of mineral dust and sea salt aerosols. *Atmospheric Chemistry and Physics*, 19, 2115–2133.
- Gupta, D., Eom, H. J., Cho, H. R., & Ro, C. U. (2015). Hygroscopic behavior of NaCl-MgCl<sub>2</sub> mixture particles as nascent sea-spray aerosol surrogates and observation of efflorescence during humidification. *Atmospheric Chemistry and Physics*, 15, 11,273–11,290.
- He, H., Wang, Y., Ma, Q., Ma, J., Chu, B., Ji, D., et al. (2014). Mineral dust and NO<sub>x</sub> promote the conversion of SO<sub>2</sub> to sulfate in heavy pollution days. *Scientific Reports*, 4, 4172. <https://doi.org/10.1038/srep04172>
- Herich, H., Tritscher, T., Wiacek, A., Gysel, M., Weingartner, E., Lohmann, U., et al. (2009). Water uptake of clay and desert dust aerosol particles at sub- and supersaturated water vapor conditions. *Physical Chemistry Chemical Physics*, 11, 7804–7809.
- Huang, J. P., Wang, T. H., Wang, W. C., Li, Z. Q., & Yan, H. R. (2014). Climate effects of dust aerosols over East Asian arid and semiarid regions. *Journal of Geophysical Research: Atmospheres*, 119, 11, 398–11,416. <https://doi.org/10.1002/2014JD021796>
- Huang, X., Song, Y., Zhao, C., Cai, X., Zhang, H., & Zhu, T. (2015). Direct radiative effect by multicomponent aerosol over China. *Journal of Climate*, 28, 3472–3495.
- Huneus, N., Schulz, M., Balkanski, Y., Griesfeller, J., Prospero, J., Kinne, S., et al. (2011). Global dust model intercomparison in AeroCom phase I. *Atmospheric Chemistry and Physics*, 11, 7781–7816.
- Ito, A., & Wagai, R. (2017). Global distribution of clay-size minerals on land surface for biogeochemical and climatological studies. *Scientific Data*, 4.
- Jian, X., Zhang, W., Liang, H., Guan, P., & Fu, L. (2019). Mineralogy, petrography and geochemistry of an early Eocene weathering profile on basement granodiorite of Qaidam basin, northern Tibet: Tectonic and paleoclimatic implications. *Catena*, 172, 54–64.
- Jickells, T. D., An, Z. S., Andersen, K. K., Baker, A. R., Bergametti, G., Brooks, N., et al. (2005). Global iron connections between desert dust, ocean biogeochemistry and climate. *Science*, 308, 67–71.
- Jordan, C. E., Pszenny, A. A. P., Keene, W. C., Cooper, O. R., Deegan, B., Maben, J., et al. (2015). Origins of aerosol chlorine during winter over north central Colorado, USA. *Journal of Geophysical Research: Atmospheres*, 120, 678–694. <https://doi.org/10.1002/2014JD022294>
- Journet, E., Balkanski, Y., & Harrison, S. P. (2014). A new data set of soil mineralogy for dust-cycle modeling. *Atmospheric Chemistry and Physics*, 14, 3801–3816.
- Karydis, V. A., Tsimpidi, A. P., Bacer, S., Pozzer, A., Nenes, A., & Lelieveld, J. (2017). Global impact of mineral dust on cloud droplet number concentration. *Atmospheric Chemistry and Physics*, 17, 5601–5621.
- Koehler, K. A., Kreidenweis, S. M., DeMott, P. J., Petters, M. D., Prenni, A. J., & Carrico, C. M. (2009). Hygroscopicity and cloud droplet activation of mineral dust aerosol. *Geophysical Research Letters*, 36, L08805. <https://doi.org/10.1029/2009GL037348>
- Koehler, K. A., Kreidenweis, S. M., DeMott, P. J., Prenni, A. J., & Petters, M. D. (2007). Potential impact of Owens (dry) Lake dust on warm and cold cloud formation. *Journal of Geophysical Research*, 112, D12210. <https://doi.org/10.11029/12007JD008413>
- Krueger, B. J., Grassian, V. H., Cowin, J. P., & Laskin, A. (2004). Heterogeneous chemistry of individual mineral dust particles from different dust source regions: The importance of particle mineralogy. *Atmospheric Environment*, 38(36), 6253–6261.
- Kumar, P., Sokolik, I. N., & Nenes, A. (2011). Measurements of cloud condensation nuclei activity and droplet activation kinetics of fresh unprocessed regional dust samples and minerals. *Atmospheric Chemistry and Physics*, 11, 3527–3541.
- Laskin, A., Iedema, M. J., Ichkovich, A., Graber, E. R., Taraniuk, I., & Rudich, Y. (2005). Direct observation of completely processed calcium carbonate dust particles. *Faraday Discussions*, 130, 453–468.
- Laskin, A., Wietsma, T. W., Krueger, B. J., & Grassian, V. H. (2005). Heterogeneous chemistry of individual mineral dust particles with nitric acid: A combined CCSEM/EDX, ESEM, and ICP-MS study. *Journal of Geophysical Research*, 110, D10208. <https://doi.org/10.1029/2004JD005206>
- Li, W. J., & Shao, L. Y. (2009). Observation of nitrate coatings on atmospheric mineral dust particles. *Atmospheric Chemistry and Physics*, 9, 1863–1871.
- Li, W. J., Shao, L. Y., Shi, Z. B., Chen, J. M., Yang, L. X., Yuan, Q., et al. (2014). Mixing state and hygroscopicity of dust and haze particles before leaving Asian continent. *Journal of Geophysical Research: Atmospheres*, 119, 1044–1059. <https://doi.org/10.1002/2013JD021003>
- Li, W. J., Xu, L., Liu, X. H., Zhang, J. C., Lin, Y. T., Yao, X. H., et al. (2017). Air pollution–aerosol interactions produce more bioavailable iron for ocean ecosystems. *Science Advances*, 3. <https://doi.org/10.1601126/sciadv.1601749>
- Ma, Q. X., He, H., & Liu, Y. C. (2010). In situ DRIFTS study of hygroscopic behavior of mineral aerosol. *Journal of Environmental Sciences*, 22, 555–560.
- Mahowald, N., Ward, D. S., Kloster, S., Flanner, M. G., Heald, C. L., Heavens, N. G., et al. (2011). Aerosol impacts on climate and biogeochemistry. *Annual Review of Environment and Resources*, 36, 45–74.

- Mahowald, N. M., Hamilton, D. S., Mackey, K. R. M., Moore, J. K., Baker, A. R., Scanza, R. A., & Zhang, Y. (2018). Aerosol trace metal leaching and impacts on marine microorganisms. *Nature Communications*, 9, 2614. <https://doi.org/10.1038/s41467-018-04970-41467>
- Martin, S. T. (2000). Phase transitions of aqueous atmospheric particles. *Chemical Reviews*, 100, 3403–3453.
- Mitroo, D., Gill, T. E., Haas, S., Pratt, K. A., & Gaston, C. J. (2019). ClNO<sub>2</sub> production from N<sub>2</sub>O<sub>5</sub> uptake on saline playa dusts: New insights into potential inland sources of ClNO<sub>2</sub>. *Environmental Science & Technology*, 13, 7442–7452.
- Murray, B. J., O'Sullivan, D., Atkinson, J. D., & Webb, M. E. (2012). Ice nucleation by particles immersed in supercooled cloud droplets. *Chemical Society Reviews*, 41, 6519–6554.
- Navea, J. G., Chen, H. H., Huang, M., Carmichael, G. R., & Grassian, V. H. (2010). A comparative evaluation of water uptake on several mineral dust sources. *Environment and Chemistry*, 7, 162–170.
- Nickovic, S., Vukovic, A., Vujadinovic, M., Djurdjevic, V., & Pejanovic, G. (2012). Technical note: High-resolution mineralogical database of dust-productive soils for atmospheric dust modeling. *Atmospheric Chemistry and Physics*, 12, 845–855.
- Nowak, S., Lafon, S., Caquineau, S., Journet, E., & Laurent, B. (2018). Quantitative study of the mineralogical composition of mineral dust aerosols by X-ray diffraction. *Talanta*, 186, 133–139.
- Osada, K. (2013). Water soluble fraction of Asian dust particles. *Atmospheric Research*, 124, 101–108.
- Pratt, K. A., Twohy, C. H., Murphy, S. M., Moffet, R. C., Heymsfield, A. J., Gaston, C. J., et al. (2010). Observation of playa salts as nuclei in orographic wave clouds. *Journal of Geophysical Research*, 115, D15301. <https://doi.org/10.1029/12009JD013606>
- Prospero, J. M., Ginoux, P., Torres, O., Nicholson, S. E., & Gill, T. E. (2002). Environmental characterization of global sources of atmospheric soil dust identified with the Nimbus 7 Total Ozone Mapping Spectrometer (TOMS) absorbing aerosol product. *Reviews of Geophysics*, 40(1), 1002. <https://doi.org/10.1029/2000RG000095>
- Rodríguez-Navarro, C., di Lorenzo, F., & Elert, K. (2018). Mineralogy and physicochemical features of Saharan dust wet deposited in the Iberian Peninsula during an extreme red rain event. *Atmospheric Chemistry and Physics*, 18, 10,089–10,122.
- Romanias, M. N., Zeineddine, M. N., Gaudion, V., Lun, X., Thevenet, F., & Riffault, V. (2016). Heterogeneous interaction of isopropanol with natural Gobi dust. *Environmental Science & Technology*, 50, 11,714–11,722.
- Rubasinghege, G., & Grassian, V. H. (2013). Role(s) of adsorbed water in the surface chemistry of environmental interfaces. *Chemical Communications*, 49, 3071–3094.
- Shao, L. Y., Li, W. J., Yang, S. S., Shi, Z. B., & Lü, S. L. (2007). Mineralogical characteristics of airborne particles collected in Beijing during a severe Asian dust storm period in spring 2002. *Science China Earth Sciences*, 50, 953–959.
- Shi, Z. B., Shao, L. T., Jones, T. P., & Lu, S. L. (2005). Microscopy and mineralogy of airborne particles collected during severe dust storm episodes in Beijing, China. *Journal of Geophysical Research*, 110, D01303. <https://doi.org/10.101029/02004JD005073>
- Sullivan, R. C., Moore, M. J. K., Petters, M. D., Kreidenweis, S. M., Roberts, G. C., & Prather, K. A. (2009). Effect of chemical mixing state on the hygroscopicity and cloud nucleation properties of calcium mineral dust particles. *Atmospheric Chemistry and Physics*, 9, 3303–3316.
- Tang, M. J., Cziczo, D. J., & Grassian, V. H. (2016). Interactions of water with mineral dust aerosol: Water adsorption, hygroscopicity, cloud condensation and ice nucleation. *Chemical Reviews*, 116, 4205–4259.
- Tang, M. J., Gu, W. J., Ma, Q. X., Li, Y. J., Zhong, C., Li, S., et al. (2019). Water adsorption and hygroscopic growth of six anemophilous pollen species: The effect of temperature. *Atmospheric Chemistry and Physics*, 19, 2247–2258.
- Tang, M. J., Huang, X., Lu, K. D., Ge, M. F., Li, Y. J., Cheng, P., et al. (2017). Heterogeneous reactions of mineral dust aerosol: Implications for tropospheric oxidation capacity. *Atmospheric Chemistry and Physics*, 17, 11,727–11,777.
- Tang, M. J., Schuster, G., & Crowley, J. N. (2014). Heterogeneous reaction of N<sub>2</sub>O<sub>5</sub> with illite and Arizona test dust particles. *Atmospheric Chemistry and Physics*, 14, 245–254.
- Tang, M. J., Thieser, J., Schuster, G., & Crowley, J. N. (2012). Kinetics and mechanism of the heterogeneous reaction of N<sub>2</sub>O<sub>5</sub> with mineral dust particles. *Physical Chemistry Chemical Physics*, 14, 8551–8561.
- Textor, C., Schulz, M., Guibert, S., Kinne, S., Balkanski, Y., Bauer, S., et al. (2006). Analysis and quantification of the diversities of aerosol life cycles within AeroCom. *Atmospheric Chemistry and Physics*, 6, 1777–1813.
- Topping, D. O., McFiggans, G. B., & Coe, H. (2005). A curved multi-component aerosol hygroscopicity model framework: Part 1—Inorganic compounds. *Atmospheric Chemistry and Physics*, 5, 1205–1222.
- Usher, C. R., Michel, A. E., & Grassian, V. H. (2003). Reactions on mineral dust. *Chemical Reviews*, 103, 4883–4939.
- Wagner, C., Schuster, G., & Crowley, J. N. (2009). An aerosol flow tube study of the interaction of N<sub>2</sub>O<sub>5</sub> with calcite, Arizona dust and quartz. *Atmospheric Environment*, 43, 5001–5008.
- Wang, G. H., Zhou, B. H., Cheng, C. L., Cao, J. J., Li, J. J., Meng, J. J., et al. (2013). Impact of Gobi desert dust on aerosol chemistry of Xi'an, inland China during spring 2009: Differences in composition and size distribution between the urban ground surface and the mountain atmosphere. *Atmospheric Chemistry and Physics*, 13, 819–835.
- Wang, H. C., Lu, K. D., Guo, S., Wu, Z. J., Shang, D. J., Tan, Z. F., et al. (2018). Efficient N<sub>2</sub>O<sub>5</sub> uptake and NO<sub>3</sub> oxidation in the outflow of urban Beijing. *Atmospheric Chemistry and Physics*, 18, 9705–9721.
- Wang, X., Hua, T., Zhang, C., Lang, L., & Wang, H. (2012). Aeolian salts in Gobi deserts of the western region of Inner Mongolia: Gone with the dust aerosols. *Atmospheric Research*, 118, 1–9.
- Wang, X. F., Wang, H., Xue, L. K., Wang, T., Wang, L. W., Gu, R. R., et al. (2017). Observations of N<sub>2</sub>O<sub>5</sub> and ClNO<sub>2</sub> at a polluted urban surface site in north China: High N<sub>2</sub>O<sub>5</sub> uptake coefficients and low ClNO<sub>2</sub> product yields. *Atmospheric Environment*, 156, 125–134.
- Wu, F., Zhang, D. Z., Cao, J. J., Xu, H. M., & An, Z. S. (2012). Soil-derived sulfate in atmospheric dust particles at Taklimakan desert. *Geophysical Research Letters*, 39, L24803. <https://doi.org/10.21029/22012GL054406>
- Wu, Z., Chen, J., Wang, Y., Zhu, Y., Liu, Y., Yao, B., et al. (2018). Interactions between water vapor and atmospheric aerosols have key roles in air quality and climate change. *National Science Review*, 5, 452–454.
- Zhang, D. Z., & Iwasaka, Y. (1999). Nitrate and sulfate in individual Asian dust-storm particles in Beijing, China in spring of 1995 and 1996. *Atmospheric Environment*, 33, 3213–3223.
- Zhang, X. Y., Gong, S. L., Zhao, T. L., Arimoto, R., Wang, Y. Q., & Zhou, Z. J. (2003). Sources of Asian dust and role of climate change versus desertification in Asian dust emission. *Geophysical Research Letters*, 30(24), 2272. <https://doi.org/10.1029/2003GL018206>
- Zhang, X. Y., Zhuang, G. S., Yuan, H., Rahn, K. A., Wang, Z. F., & An, Z. S. (2009). Aerosol particles from dried salt-lakes and saline soils carried on dust storms over Beijing. *Terrestrial, Atmospheric and Oceanic Sciences*, 20, 619–628.
- Zhou, W., Zhao, J., Ouyang, B., Mehra, A., Xu, W., Wang, Y., et al. (2018). Production of N<sub>2</sub>O<sub>5</sub> and ClNO<sub>2</sub> in summer in urban Beijing, China. *Atmospheric Chemistry and Physics*, 18, 11,581–11,597.
- Zhu, B. Q. (2016a). Atmospheric significance of aeolian salts in the sandy deserts of northwestern China. *Solid Earth*, 7, 191–203.
- Zhu, B. Q. (2016b). Hydrological indications of aeolian salts in mid-latitude deserts of northwestern China. *Journal of Earth System Science*, 125, 809–820.